



UNIVERSITY OF LEEDS

This is a repository copy of *IGF signalling and endocytosis in the human villous placenta in early pregnancy as revealed by comparing quantum dot conjugates with a soluble ligand*.

White Rose Research Online URL for this paper:
<http://eprints.whiterose.ac.uk/147471/>

Version: Accepted Version

Article:

Karolczak-Bayatti, M, Forbes, K orcid.org/0000-0002-3745-1337, Horn, J et al. (4 more authors) (2019) IGF signalling and endocytosis in the human villous placenta in early pregnancy as revealed by comparing quantum dot conjugates with a soluble ligand. *Nanoscale*, 11 (25). pp. 12285-12295. ISSN 2040-3364

<https://doi.org/10.1039/C8NR10337B>

© The Royal Society of Chemistry 2019. This article is protected by copyright. This is an author produced version of a paper published in *Nanoscale*. Uploaded in accordance with the publisher's self-archiving policy.

Reuse

Items deposited in White Rose Research Online are protected by copyright, with all rights reserved unless indicated otherwise. They may be downloaded and/or printed for private study, or other acts as permitted by national copyright laws. The publisher or other rights holders may allow further reproduction and re-use of the full text version. This is indicated by the licence information on the White Rose Research Online record for the item.

Takedown

If you consider content in White Rose Research Online to be in breach of UK law, please notify us by emailing eprints@whiterose.ac.uk including the URL of the record and the reason for the withdrawal request.



eprints@whiterose.ac.uk
<https://eprints.whiterose.ac.uk/>

IGF signalling and endocytosis in the human villous placenta in early pregnancy as revealed by comparing quantum dot conjugates with soluble ligand

^{1,2}Magdalena Karolczak-Bayatti, ^{1,2}Karen Forbes, ^{1,2}James Horn, ^{3,4}Tambet Teesalu, ^{1,2}Lynda K Harris, ^{1,2}Melissa Westwood, ^{1,2}John D Aplin

¹Maternal and Fetal Health Research Centre, School of Medical Sciences, University of Manchester, Manchester Academic Health Sciences Centre, St Mary's Hospital, Manchester M13 9WL, UK.

²Maternal and Fetal Health Research Centre, Manchester University NHS Foundation Trust, Manchester Academic Health Sciences Centre, St Mary's Hospital, Manchester M13 9WL, UK.

³Laboratory of Cancer Biology, Institute of Biomedicine, Centre of Excellence for Translational Medicine, University of Tartu, Ravila 14b, Tartu 50411, Estonia.

⁴Cancer Research Center, Sanford-Burnham-Prebys Medical Discovery Institute, 10901 North Torrey Pines Road, La Jolla, CA 92037, USA

Abstract

A complex combination of trafficking and signalling occurs at the surface of the placenta. The system delivers maternal nutrients to the fetus and facilitates gaseous exchange, whilst mediating signal transduction to support and stimulate the growth of the placenta itself. IGF-I is acknowledged as a maternally-derived ligand important in the regulation of placental growth. Here we show that quantum dots bearing IGF can stimulate IGF receptor (IGF1R) phosphorylation in the syncytio- (maternal-facing) and cyto- (fetal-facing) trophoblast bilayer that forms the outer boundary of the placenta, in a distribution similar to the one resulting from exposure to soluble ligand. The conjugates are internalised by a clathrin-dependent pathway and delivered to a syncytioplasmic compartment that differs from conventional late endosomes and lysosomes. Two discrete downstream responses are evident in different cellular compartments: phosphorylation of P70S6K in the non-proliferative syncytiotrophoblast and of AKT in cytotrophoblast. Co-conjugation of IGF-quantum dots with an RGD-containing ligand permits penetration beyond the syncytium, into the cytoplasm of the underlying cytotrophoblast. These data reveal the existence of a trans-syncytial pathway that allows maternal mitotic signals to penetrate to the inner progenitor cells, which must proliferate to support placental and consequently fetal growth.

Introduction

In vivo studies, most notably in mouse and guinea pig, have demonstrated a central role for the insulin-like growth factors (IGFs) in normal development of the placenta.¹ *In vitro*, application of IGF-I or -II to the maternal-facing microvillous

membrane (MVM) of the syncytiotrophoblast in human early placental explants affects underlying cytotrophoblast by increasing mitosis and inhibiting apoptosis (Figure 1).² The type 1 IGF-I receptor (IGF1R) is present both on the MVM and cytotrophoblast, therefore in principle, maternal IGFs could act on either or both cell populations to influence the trophoblast life cycle and capacity for placental expansion. However, the signalling mechanisms that underlie IGF actions in the placenta are not known.

View Article Online
DOI: 10.1039/C8NR10337B

In the current study, we use intact human placental explants to show that IGF-I activates signalling events in both trophoblast layers. We further use a pharmacological approach to suggest that signal transduction is linked to clathrin-mediated endocytosis. We go on to exploit quantum dot (QD)-conjugated IGF-I to investigate binding, intracellular turnover and downstream signalling of IGF-I and IGF1R in syncytium and cytotrophoblast. We examine subcellular localisation of the signal over time and investigate its trans-syncytial transmission to the underlying cytotrophoblast layer.

We have recently demonstrated that the tumour homing peptide iRGD (CRGDKGPDC) can be exploited to selectively deliver payloads such as IGF-I to placental tissue in mice and humans.³ This well-characterised cyclic peptide binds to αv integrins and neuropilin-1 on the surface of tumour cells, facilitating rapid internalization;^{4, 5} both of these receptors are present on the placental microvillous membrane.^{6, 7} To explore this alternative binding modality and its downstream consequences in the early placenta, we address QDs with a combination of IGF-I and iRGD, and compare the respective internalisation and signalling pathways taken by these bifunctional particles.

Experimental

Tissue

First-trimester (6 - 8 gestational weeks) placentas were obtained by elective surgical termination of pregnancy. All tissue was collected with informed maternal consent in accordance with Local Ethics Committee approval. Placental explants (2-3mm³) comprised of small cluster of terminal villous branches, were cultured in DMEM/F12 serum-free medium supplemented with 4mM glutamine, 100 μ g/L streptomycin and 100U/L penicillin for 24h to allow a decrease in endogenous intracellular signalling prior to IGF-I treatment.² If significant residual phosphorylation of AKT was still evident after this time (determined by Western blotting of tissue lysates) the data were not further utilised. Note that residual pAKT may have arisen from cells in either trophoblast or stroma; the stromal signalling noted in immunofluorescence analyses was not an impediment to studying signal transduction in trophoblast. Tissues from all experiments were examined carefully by histology for evidence of syncytial delamination, blebbing or other signs of degeneration. Such features were rarely seen, and small areas of the epithelium with signs of reduced viability could always be avoided. Neither did we observe syncytial regeneration, which can occur in late pregnancy explant cultures after sloughing (PMID 11247834). Folding

together of villi could potentially cause reduced access of nanoparticles to some areas of the villous surface, and indeed IGF stimulation (receptor phosphorylation at the microvillous membrane) was evident, but not in all parts of the syncytial surface. We did not observe accumulation of QDs at the cut surfaces of tissue; by far the majority of particles were adherent to or interacting with trophoblast.

IGF labelling and treatment

Biotinylated IGF-I (GroPep) was loaded on streptavidin-conjugated quantum dots (QD; QD 655, Invitrogen; <https://www.thermofisher.com/order/catalog/product/Q10123MP>) in 2.5:1 molar ratio. The QD (CdSe nanocrystals coated with a ZnS shell, then further coated with a derivatisable polymer) are ~15–20 nm in diameter and we estimate a mean of 9 IGF ligand molecules were reacted per particle. If iRGD peptide (CRB Cambridge) was included in the complex, IGF-I, QD and iRGD peptide were used in 2.5:1:1 molar ratio. As IgG is internalized into the syncytium via an unrelated pathway,^{8,9} we used biotinylated IgG (Rockland Antibodies and Assays) conjugated to QD as well as unconjugated QDs as controls. Labelling was carried out by incubating, with shaking, in 10 mM TRIS-Cl at 4°C for 1h. Non-conjugated molecules were removed using Micro Bio-Spin chromatography columns (BioRad). Explants were incubated with vehicle, IGF-I (20nM), biotinylated IGF-I (50nM), QD-IGF-I / QD-IgG (50 or 100 nM protein) or QD-iRGD-IGF-I / QD-iRGD-IgG (50 or 100 nM IGF/IgG) for 30 min to 24 h. In some experiments, explants were pretreated for 1 hour with an inhibitor of clathrin-dependent (100µM chlorpromazine (CPMZ), Sigma) or caveolin-dependent (5mM methyl-β-cyclodextrin (β-MCD), or 10µg/ml filipin, both Sigma) endocytosis, or cytochalasin D (10µM; 1:1000 from a DMSO stock solution). Then, IGF-I (20 nM) treatment was carried out in inhibitor-free medium.

Fluorescence Immunohistochemistry

Cultured placental explants were fixed in 4% paraformaldehyde for 2h, then transferred to phosphate-buffered saline (PBS) for 24h. Samples were embedded in paraffin or in OCT (for QD localisation), sectioned (5µm), and mounted on glass slides. Paraffin embedded sections were dewaxed in xylene and rehydrated. Antigen retrieval was performed by boiling in 0.1 M sodium citrate buffer, pH 6.3 for 10 min or by incubating in 2mM EDTA pH 6.0 at 80°C for 20 min (Table 1). Tissues were treated with sodium borohydride (10mg/ml, 3x10min), followed with a PBS wash, to decrease syncytial autofluorescence, then incubated with primary antibody overnight at 4°C and with fluorescent secondary antibody for 1h at room temperature (Table 1). Images were taken using the Zen imaging system (Zeiss). Control experiments included omission of primary or secondary antibodies, or substitution of primary antibody with mouse or rabbit IgG.

Western Blotting

Placental tissues were homogenized in sucrose buffer (62.5 TRIS-CL pH 6.8, 2% SDS, 10% sucrose and phosphatase inhibitors). Protein concentration was determined using the DC protein assay (BioRad) and 20 µg of total protein were separated on a 10% polyacrylamide-SDS gel. Proteins were transferred using wet transfer to nitrocellulose membranes. Non-specific signal was blocked by incubating

membranes in 5% fat-free milk, 5% BSA or, for phospho-specific antibodies (GenDepot), West-EZier Super Blocking buffer for 30 min (Table 2). Membranes were incubated with primary antibody (Table 2) overnight, at 4°C then signal was detected using HRP- or fluorescence-labelled secondary antibodies.

View Article Online
DOI: 10.1039/C8NR10337B

Statistics

The level of phosphorylated proteins was normalized against total levels of respective protein and expressed as a fold-change versus vehicle-treated samples. Changes in the level of protein activation were assessed using Kruskal-Wallis followed by Dunn's post hoc test.

Results

IGF-I signalling in first trimester placenta

Treatment of placental explants with IGF-I led to phosphorylation of IGF-1R (Figure 2), initially in the syncytial microvillous membrane (apparent after 5 minutes) and then in cytotrophoblast (15 and 30 minutes, with a decline apparent at the later time). Immunohistochemical analysis of downstream signalling molecules revealed that IGF-I treatment resulted in redistribution of pP70S6K from the cytoplasm to the apical (microvillous) and basal membranes of the syncytium, whereas pP70S6K was absent from cytotrophoblast (Figure 3). In contrast, IGF-I-stimulated activation of AKT was observed only in cytotrophoblast. These data indicate that after IGF-I binding to the 'maternal' surface of the trophoblast bilayer, signalling via P70S6K occurs in the syncytium, and a trans-syncytial signal is transmitted to underlying cytotrophoblast.

IGF-I signalling is dependent on clathrin-mediated endocytosis

The role of endocytosis in signalling events downstream of IGF1R was investigated by western blot analysis of phosphoforms following IGF-I stimulation of explants pretreated with endocytosis inhibitors (Figure 4). CPMZ, used to inhibit clathrin-dependent endocytosis, did not affect IGF1R phosphorylation, suggesting that receptor activation can occur efficiently at the cell surface even if clathrin-mediated internalisation is impaired. Nevertheless, CPMZ decreased IGF-I mediated phosphorylation of AKT ($p < 0.0001$), P70S6K ($p = 0.038$) and GSK ($p = 0.003$) (Figure 4), suggesting that these intracellular pathways may be activated after clathrin-mediated internalisation of IGF-I. β -MCD and filipin, inhibitors of caveolin-mediated endocytosis, did not affect IGF-I stimulated phosphorylation of IGF1R or activation of the AKT, p70S6K and pGSK pathways (Supp Fig 1), consistent with lack of caveolin in first trimester placenta.¹⁰

QD-IGF conjugates induce phosphorylation of IGF1R

Next, we wished to investigate whether IGF-I translocates through the trophoblast bilayer and whether ligand location influences signalling using QD-IGF. In addition, QD-IGF was conjugated to the placental homing peptide iRGD, which binds integrin $\alpha v \beta 3$ and, after proteolytic cleavage, the co-receptor neuropilin-1⁵ (both shown to

be expressed in the MVM in Figure 6), to determine if changing the repertoire of potential extracellular binding partners might affect intracellular signalling and translocation. Initial experiments to assess the biological activity of the IGF conjugates confirmed that both QD-IGF-I and QD-IGF-I-peptide are able to activate the IGF receptor (Figure 5). However the control conjugate, QD-IgG, did not stimulate IGF1R, in keeping with the notion that placental internalisation of IgG⁸ does not activate phosphorylation cascades.^{11, 12} Interestingly, preventing QD-IGF-I-peptide internalisation using an antibody that blocks binding of iRGD to neuropilin-1 augmented phosphorylation of IGF1R in response to QD-IGF-I-peptide (Figure 6).

QD-IGF-I-peptide is internalised and delivered to cytotrophoblasts

QD-IGF-I particles moved from the syncytial MVM into the syncytioplasm during the first two hours of exposure, and then accumulated in the syncytioplasm (Figure 7 D-F) such that at 24h, QD-IGF-I was found throughout the syncytial layer and close to the basal surface, but penetration of the cytotrophoblast (revealed by E-cadherin staining, Figure 7F) was not observed. In contrast, QD-IGF-I conjugated to iRGD peptide was able to access the cytotrophoblast cytoplasm (Figure 7J), seen in some but not all cytotrophoblasts. Incorporation of peptide did not alter trafficking of QD-IgG, which accessed only the syncytioplasm (Figure 7G,H,I,K). Internalisation of IGF-I labeled with an alternative marker, biotin, occurred over a faster timeframe (30 minutes; Figure 7L), though subsequent observations were similar to those made with QD-IGF-I. From 2h to 24h, biotinylated IGF-I was located throughout the syncytium, but not in cytotrophoblasts (Figure 7M, N).

QD-IGF-I colocalises with IGF1R and endocytosis markers

The endocytic pathway involved in QD-IGF-I internalisation by syncytiotrophoblast was determined by assessing colocalisation with IGF1R, caveolin, clathrin and early endosomal markers (Figure 8A-D). QD-IGF-I colocalised with IGF1R and clathrin in areas at or close to the apical microvillous membrane. Surprisingly, no colocalisation was observed with the early endosomal marker EEA1, nor with Rab11a (recycling endosomes). Caveolin 1 (not shown) was not detected in trophoblast in first trimester placental tissue, though we confirmed previous reports that it is present in villous trophoblast in term human placenta. QD-IGF-I located in the mid and basal syncytium did not colocalise with any of the endosomal markers that were tested. Control QD-IgG did not colocalise with IGF1R or clathrin (Figure 8E, F).

Discussion

Earlier work showed that IGF-I can bind to the outer syncytial MVM of first trimester placenta and elicit a proliferative response in the inner cytotrophoblast layer (Figure 1).² Here we start to unpick the signalling pathway that connects these two events, combining ligand with two fluorescent nanoparticle conjugates that give novel insight into placental internalisation pathways accessible from the maternal side of the barrier. QD conjugates were used for optimal detection sensitivity as well as the relative ease of single and double ligand conjugation. Using an experimental design in which endogenous signalling was first allowed to die away during an overnight

incubation at 4 degrees in the absence of growth factors, we demonstrate that free IGF-I and biotinylated IGF-I bound to QD in the presence or absence of a co-conjugated RGD peptide can all stimulate rapid IGF1R phosphorylation in the MVM. Measures that delay internalisation of bound ligand, including pharmacological inhibition of the clathrin pathway, inhibit phosphorylation; conversely, immunological inhibition of neuropilin-1 (which is needed for internalisation of the iRGD ligand) enhanced phosphorylation, possibly by prolonging IGF-I-IGF1R interaction, and thus delaying the processes of internalisation and deactivation. These data also demonstrate that the previously defined CendR pathway,⁴ which describes how peptides bearing R/KXXR/K motifs are internalised, operates within the human placenta and could be exploited to enhance growth factor delivery, for example in pregnancies compromised by inadequate placental growth and function.

View Article Online
DOI: 10.1039/C8NR10337B

Quantum dots have been used to deliver and track a range of molecules, such as growth factors, antibodies and drugs, in a variety of tissues and organs.¹³ Tracking of QD-IGF-I delivered to the syncytial microvillous membrane demonstrates that the particles are internalised by endocytosis, in the same way as the dissolved ligand biotin-IGF-I. Thus, conjugation of IGF-I to a QD carrier alters neither its pathway of internalisation nor its ability to deliver a signal.

Based on co-localisation with clathrin, as well as pharmacological inhibition, internalisation of IGF1R occurs through clathrin-coated pits, which are well-described in the syncytial microvillous membrane.¹⁴ IGF1R is distributed in vesicular compartments throughout the syncytioplasm,¹⁵ but only co-localises with clathrin at, and immediately adjacent to, the MVM. The distribution of pIGF1R suggests that the receptor continues to signal after internalisation. However shortly after pinching off from the MVM, QDs appear to become incorporated into a transcytotic pathway that lacks conventional markers of endosomes and remains very poorly characterized.¹⁶ They eventually become concentrated in the basal syncytioplasm adjacent to the boundary between syncytium and underlying cytotrophoblast. QD-IGF-I remained entirely in the syncytioplasm up to 24h – we never observed it within the E-cadherin-labelled cytotrophoblast boundary membrane. In the case of QD-IGF-I-iRGD, we obtained evidence of transport into the cytotrophoblast cytoplasm, although this was not widespread and occurred only at 24h. However we reliably observed pIGF1R in cytotrophoblast membranes in response to both conjugates (but not QD-IgG), demonstrating that an activation signal is delivered from syncytiotrophoblast. The transcytosis route of IGF-I from the microvillous membrane to cytotrophoblasts requires further investigation, and more work is required to dissect signalling events occurring at the basal syncytiotrophoblast.

Activation of IGF1R in cytotrophoblast is followed by phosphorylation of mitotic-related signalling pathways (pAKT and pGSK). Meanwhile in the syncytium a distinct signalling cascade is initiated from IGF1R, leading to phosphorylation and redistribution to the membrane of pP70S6K, suggesting there may be stimulation of protein synthesis in syncytium.

Deficient IGF signalling is clearly associated with fetal growth restriction.^{17, 18} Though peptide targeting provides a way to specify the tissue destination of circulating nanoparticles,¹⁹ it is not likely that the present generation of QDs can serve a therapeutic function because of their trace element content, and the possibility of delivering damage signals to the fetus.^{20, 21} However, biocompatible nanocarriers including liposomes^{3, 22} are showing promise as effective delivery vehicles for growth factors and drugs to the placenta. The present data emphasise the potential for targeted delivery to achieve therapeutic effects, as well as highlighting methodology that is useful for tracing nanoparticles and evaluating the mechanistic effects of their cargoes. We demonstrate that with a novel combination of ligands and carrier, signaling entities can be delivered not just to the syncytiotrophoblast outer barrier, but also to the inner cytotrophoblast progenitor cell population of the placenta. Once pregnancies at risk of growth restriction can be reliably identified in the first trimester,²³ improving placental growth may provide a benign path to achieving more efficient nutrient transfer at a time when it is still possible to restore the growth trajectory of the fetus to normal.

Conflicts of interest

There are no conflicts of interest to declare.

Acknowledgements

This work was funded by a grant from the UK Medical Research Council (MR/J000965/1). T. Teesalu was supported by European Regional Development Fund (Project No. 2014-2020.4.01.15-0012) and Estonian Research Council grant PRG230. We thank Dr. C. Patrick Case for stimulating interaction. We are grateful to patients, nurses and doctors at St Mary's Hospital, Manchester who generously supported the study by providing placental tissue.

Figure legends

Figure 1: Diagram showing a cross-sectional view of first trimester human placenta

Figure 2: IGF-I phosphorylates syncytial, then cytotrophoblast IGF1R. (A) Control untreated tissue. (B) Rapid (5 minutes) phosphorylation of syncytial IGF1R (green, shown by arrow) was observed following treatment of first trimester placenta with IGF-I (20nM). This was followed by activation in cytotrophoblast (identified using e-cadherin (red)) after 15 (C) and 30 minutes (D) by which time activation of syncytial IGF1R had dissipated. st - syncytium, ct - cytotrophoblasts, MVM - microvillous membrane, IVS – intervillous space. Nuclei stained with DAPI (blue). Representative

images from n=3 placentas. Syncytium is enclosed by white dashed lines. Scale bar 10 μ m. [View Article Online](#)
DOI: 10.1039/C8NR10337B

Figure 3: IGF-I activation of intracellular signalling molecules in human first trimester placenta

Treatment with IGF-I (20nM) for 5 and 30 min activates intracellular AKT, GSK and P70S6K signalling pathways. Phosphorylated AKT (pAKT; A-C, n=5) was observed only in cytotrophoblasts (green, indicated by arrow). IGF-I stimulation led to pP70S6K (green, n=3) translocation from cytoplasm to the apical and basal syncytial membranes (D-F). No activation of P70S6K was observed in cytotrophoblasts. st - syncytium, ct - cytotrophoblasts, also indicated by white arrows in A, B and C. MVM - microvillous membrane, IVS - intervillous space; E-cadherin, a cytotrophoblast marker (red); DAPI, nuclear stain (blue). Representative images from n=3-5 placentas. Syncytium is enclosed by white dashed lines in A,B,C and F. Only the apical microvillous membrane is dashed in B and E to avoid obscuring the staining. In E, the basal and apical syncytiotrophoblast are marked by arrows. Scale bar, 10 μ m.

Figure 4. Clathrin-mediated endocytosis affects IGF-I induced signalling in human early placenta.

Western blot analysis of first trimester placental explant lysates (A) demonstrates that treatment with IGF-I (20nM) for 30 min increases activation of IGF1R (B; p=0.33) and AKT (C; p=0.38); control (C) vs IGF. Pretreatment for 30 min with the clathrin-mediated endocytosis inhibitor, CPMZ (100 μ M), reduces IGF-I-stimulated phosphorylation of AKT (C; p<0.0001), P70S6K (D; p=0.038) and GSK (E; p=0.003), but does not affect phosphorylation of IGF1R (B; p=0.99); IGF vs IGF+CPMZ. n=4 for pIGF1R, n=9 for pAKT, n=6 for pp70S6K and n=5 for pGSK). Within each experiment, all samples were run on the same gel; however, we have rearranged some lanes (indicated by dotted line) from the resultant image of the autoradiograph in order to present the data in the sequence used to report all other results: control, IGF, control + CPMZ, and control + IGF. Each lane contains 20 μ g protein.

Figure 5. QD-IGF-I conjugates retain biological activity.

First trimester placenta was treated for 30 minutes with QD-peptide (iRGD), QD-IGF-I (100nM), QD-IGF-I-peptide (100nM), QD-IgG (100nM) or QD-IgG-I-peptide (100nM) (concentration in brackets refers to IGF-I final concentration). 50nM IGF-biotin was used as a positive control, and untreated tissue was used to define basal levels of IGF1R phosphorylation. Western blot analysis (20 μ g protein/lane) reveals an increase in pIGF1R following treatment with QD-IGF-I-peptide (p=0.0004, n=6) and IGF-I-biotin (p=0.0005, n=4).

Figure 6. Blocking QD-IGF-I-peptide binding to neuropilin-1 increases phosphorylation of IGF1R.

Neuropilin-1 (green) is present in both the MVM and the cytotrophoblast layer, whereas integrin α / β 3 (green) is present exclusively in the MVM in the first trimester placenta (A). MVM - microvillous membrane, IVS - intervillous space, st - syncytiotrophoblast, ct - cytotrophoblast. First trimester explants were treated with

a control antibody or an antibody (10 or 20 $\mu\text{g/ml}$) specific to the neuropilin-1 iRGD peptide binding site for 1h, then incubated in the absence or presence of QD-IGF-I-peptide (iRGD) for 30 min. Activation of IGF1R was assessed by Western blotting (B). Control vs QD-IGF-I-peptide ($p=0.0099$; $n=6$) and control vs neuropilin/QD-IGF-I-peptide ($p=0.0295$; $n=3$). No difference was detected at the higher dose. Syncytium is enclosed by white dashed lines. The basal cytotrophoblast surface is also marked by a white dashed line.

Figure 7. Internalised IGF-I is delivered to cytotrophoblasts

Internalisation of free QD, QD-IGF-I and QD-IgG conjugates (red, A-I) was observed as early as 30min (A, D, G) and 2h (B, E, H) after start of the treatment. After 24h, free QD and QD-IgG conjugates were dispersed throughout the syncytioplasm, whereas QD-IGF-I were localised mainly at the basal membrane of the syncytium. Neither free QD nor IGF/IgG-QD conjugates crossed to cytotrophoblasts after 24h ($n=9$)(C, F, I). In contrast QD-IGF-I-peptide (iRGD) was observed to cross to cytotrophoblasts ($n=3$) (J^1, J^2, J^3 , each image representing a different experiment); however, addition of the iRGD peptide to the QD-IgG had no similar effect (K). Similar to QD-IGF, free IGF-I-biotin (30min-24h) was present throughout syncytium but was not observed in the cytotrophoblast layer (L-N). st - syncytium, ct - cytotrophoblasts, IVS – intervillous space; E-cadherin, a cytotrophoblast marker (green A-K); DAPI, nuclear stain (blue). Representative images from 9 experiments. In A-K the white dashed line marks the syncytial apical microvillous membrane. In L-N the syncytium is enclosed by white dashed lines.

Figure 8. Colocalisation of QD-IGF-I with IGF1R and endocytosis markers

QD-IGF-I (red) colocalised with IGF1R (A, green; arrow) and clathrin (B, green) close to the apical microvillous membrane (MVM) in the syncytial (st) but not cytotrophoblast layer (ct). This was not observed for the control QD-IgG (E and F). QD-IGF-I did not colocalise with the early endosomal marker EEA1 (C and D), or Rab11a (recycling endosome). Nuclei are stained with DAPI (blue). Representative images from $n=3$ placentas. White dashed lines delineate the apical syncytial microvillous membrane.

Table 1: Antibodies and antigen retrieval method for Immunohistochemistry View Article Online
DOI: 10.1039/C8NR10337B

Antibody	Company	Item code	Dilution	Embedding	Retrieval
pIGF1R	Invitrogen	44804	1:200	Paraffin/OCT	EDTA
IGF1R β	SantaCruz		1:200	Paraffin/OCT	EDTA
pMAPK	Cell Signalling	4370	1:100	paraffin	EDTA
pAKT	Cell Signalling	4051	1:100	paraffin	EDTA
pP70s6k	Cell Signalling	9234	1:100	paraffin	EDTA
pGSK-3B	Cell Signalling	5558P	1:100	paraffin	EDTA
mCaveolin	BD	610406	1:100	OCT	N/A
Neuropilin-1	Abcam	Ab81321		OCT	N/A
Rab11a	BD		1:100	OCT	N/A
mEEA1	BD	610456	1:100	OCT	N/A
clathrin	BD	610499	1:100	OCT	N/A
aV/B3	Millipore	MAB19762		OCT	N/A
Transferin receptor	Abcam	84086	1:100	OCT	N/A
mouse e-cadherin	BD	610182	1:400	OCT/paraffin	N/A
rabbit e-cadherin	Cell Signalling	3195P	1:500	OCT/paraffin	N/A
Anti-rabbit or anti-mouse secondary Ab Alexa 488	Invitrogen	A-21206 A-21202	1:500	OCT/paraffin	N/A
Anti-rabbit or anti-mouse secondary Ab Alexa 568	Invitrogen	A-10042 A-10037	1:500	OCT/paraffin	N/A

Table 2. Antibodies used for Western blotting

Antibody	Company	Item code	Antibody dilution	Blocking / Incubation buffer	Detection method
pMAPK	Cell Signalling	4370	1:250	5%/1% milk solids	LI-COR
MAPK	Cell Signalling	9102	1:500	5%/1% milk	LI-COR
pAKT	Cell Signalling	4060	1:250	5%/1% milk	LI-COR
AKT	Cell Signalling	9272	1:500	5%/1% milk	LI-COR
p-p70S6K	Cell Signalling	9234	1:500	EZier	HRP
p70S6K	Cell Signalling	2708	1:500	EZier	HRP
pIGF1R	Cell Signalling	3021	1:250	EZier	HRP
IGF1R β	Santa Cruz			milk	LI-COR
pGSK	Cell Signalling	D85E12	1:500	5%/1% BSA	HRP
GSK-3 β	Cell Signalling	D5C5Z	1:500	5%/1% BSA	HRP
HRP-conjugated anti-Rabbit IgG	DAKO	P0448	1:5000	1% milk	
HRP-conjugated anti-mouse IgG	DAKO	P0447	1:5000	1% milk	
Fluorescently labelled anti-mouse IgG	LI-COR	926-68073	1:10000	1% milk	
Fluorescently labelled anti-rabbit IgG	LI-COR	926-32213	1:10000	1% milk	

1. C. T. Roberts, J. A. Owens and A. N. Sferruzzi-Perri, *Placenta*, 2008, **29 Suppl A**, S42-47.
2. K. Forbes, M. Westwood, P. N. Baker and J. D. Aplin, *Am J Physiol Cell Physiol*, 2008, **294**, C1313-C1322.
3. A. King, C. Ndifon, S. Lui, K. Widdows, V. R. Kotamraju, L. Agemy, T. Teesalu, J. D. Glazier, F. Cellesi, N. Tirelli, J. D. Aplin, E. Ruoslahti and L. K. Harris, *Sci Adv*, 2016, **2**, e1600349.
4. T. Teesalu, K. N. Sugahara, V. R. Kotamraju and E. Ruoslahti, *Proceedings of the National Academy of Sciences of the United States of America*, 2009, **106**, 16157-16162.
5. K. N. Sugahara, T. Teesalu, P. P. Karmali, V. R. Kotamraju, L. Agemy, O. M. Girard, D. Hanahan, R. F. Mattrey and E. Ruoslahti, *Cancer Cell*, 2009, **16**, 510-520.
6. Z. Kertesz, E. A. Linton and C. W. Redman, *Placenta*, 2000, **21**, 150-159.

7. D. M. Baston-Buest, A. C. Porn, A. Schanz, J. S. Kruessel, W. Janni and A. P. Hess, *Eur J Obstet Gynecol Reprod Biol*, 2011, **154**, 151-156. View Article Online
DOI: 10.1039/C8NR10337B
8. N. E. Simister, C. M. Story, H. L. Chen and J. S. Hunt, *Eur J Immunol*, 1996, **26**, 1527-1531.
9. J. L. Leach, D. D. Sedmak, J. M. Osborne, B. Rahill, M. D. Lairmore and C. L. Anderson, *J Immunol*, 1996, **157**, 3317-3322.
10. T. W. Lyden, C. L. Anderson and J. M. Robinson, *Placenta*, 2002, **23**, 640-652.
11. S. V. Kane and L. A. Acquah, *Am.J Gastroenterol.*, 2009, **104**, 228-233.
12. E. S. Ward and R. J. Ober, *Trends Pharmacol Sci*, 2018, **39**, 892-904.
13. C. E. Probst, P. Zrazhevskiy, V. Bagalkot and X. Gao, *Adv Drug Deliv Rev*, 2013, **65**, 703-718.
14. C. J. Jones and H. Fox, *Electron Microsc Rev*, 1991, **4**, 129-178.
15. K. Forbes, V. K. Shah, K. Siddals, J. M. Gibson, J. D. Aplin and M. Westwood, *Mol Hum Reprod*, 2015, **21**, 105-114.
16. K. Y. Y. Fung, G. D. Fairn and W. L. Lee, *Traffic*, 2018, **19**, 5-18.
17. R. Randhawa and P. Cohen, *Mol Genet Metab*, 2005, **86**, 84-90.
18. L. Laviola, S. Perrini, G. Belsanti, A. Natalicchio, C. Montrone, A. Leonardini, A. Vimercati, M. Scioscia, L. Selvaggi, R. Giorgino, P. Greco and F. Giorgino, *Endocrinology*, 2005, **146**, 1498-1505.
19. E. Ruoslahti, *Adv Mater*, 2012, **24**, 3747-3756.
20. E. Mansell, N. Zareian, C. Malouf, C. Kapeni, N. Brown, C. Badie, D. Baird, J. Lane, K. Ottersbach, A. Blair and C. P. Case, *Sci Rep*, 2019, **9**, 4370.
21. A. Sood, S. Salih, D. Roh, L. Lacharme-Lora, M. Parry, B. Hardiman, R. Keehan, R. Grummer, E. Winterhager, P. J. Gokhale, P. W. Andrews, C. Abbott, K. Forbes, M. Westwood, J. D. Aplin, E. Ingham, I. Papageorgiou, M. Berry, J. Liu, A. D. Dick, R. J. Garland, N. Williams, R. Singh, A. K. Simon, M. Lewis, J. Ham, L. Roger, D. M. Baird, L. A. Crompton, M. A. Caldwell, H. Swalwell, M. Birch-Machin, G. Lopez-Castejon, A. Randall, H. Lin, M. S. Suleiman, W. H. Evans, R. Newson and C. P. Case, *Nat Nanotechnol*, 2011, **6**, 824-833.
22. N. Cureton, I. Korotkova, B. Baker, S. Greenwood, M. Wareing, V. R. Kotamraju, T. Teesalu, F. Cellesi, N. Tirelli, E. Ruoslahti, J. D. Aplin and L. K. Harris, *Theranostics*, 2017, **7**, 3715-3731.
23. G. C. S. Smith, *Best practice & research. Clinical obstetrics & gynaecology*, 2018, **49**, 16-28.

Figure 1

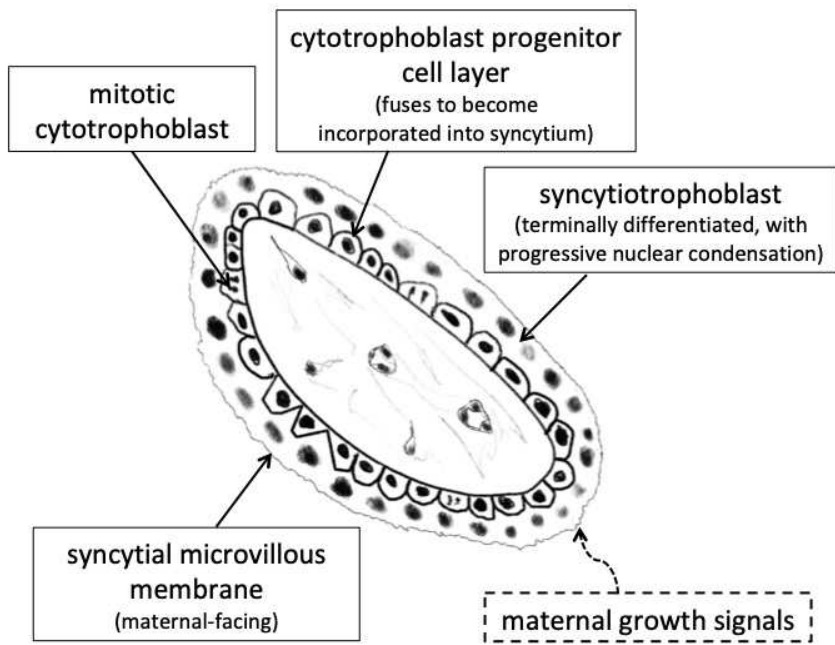


Figure 1: Diagram showing a cross-sectional view of first trimester human placenta

254x338mm (72 x 72 DPI)

Published on 06 June 2019. Downloaded by University of Leeds on 6/17/2019 9:20:14 PM.

Nanoscale Accepted Manuscript

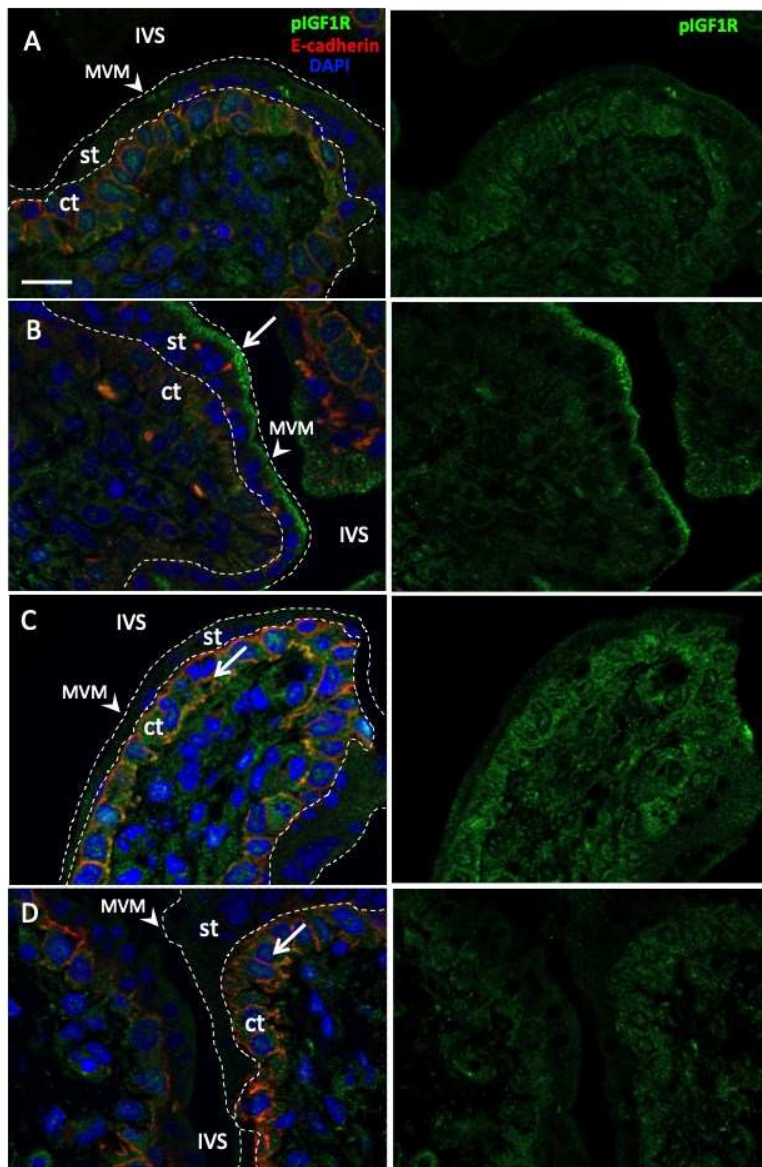


Figure 2

Figure 2: IGF-I phosphorylates syncytial, then cytotrophoblast IGF1R. (A) Control untreated tissue. (B) Rapid (5 minutes) phosphorylation of syncytial IGF1R (green, shown by arrow) was observed following treatment of first trimester placenta with IGF-I (20nM). This was followed by activation in cytotrophoblast (identified using e-cadherin (red)) after 15 (C) and 30 minutes (D) by which time activation of syncytial IGF1R had dissipated. st - syncytium, ct - cytotrophoblasts, MVM - microvillous membrane, IVS - intervillous space. Nuclei stained with DAPI (blue). Representative images from n=3 placentas. Syncytium is enclosed by white dashed lines. Scale bar, 10 μ m.

254x338mm (72 x 72 DPI)

Figure 3

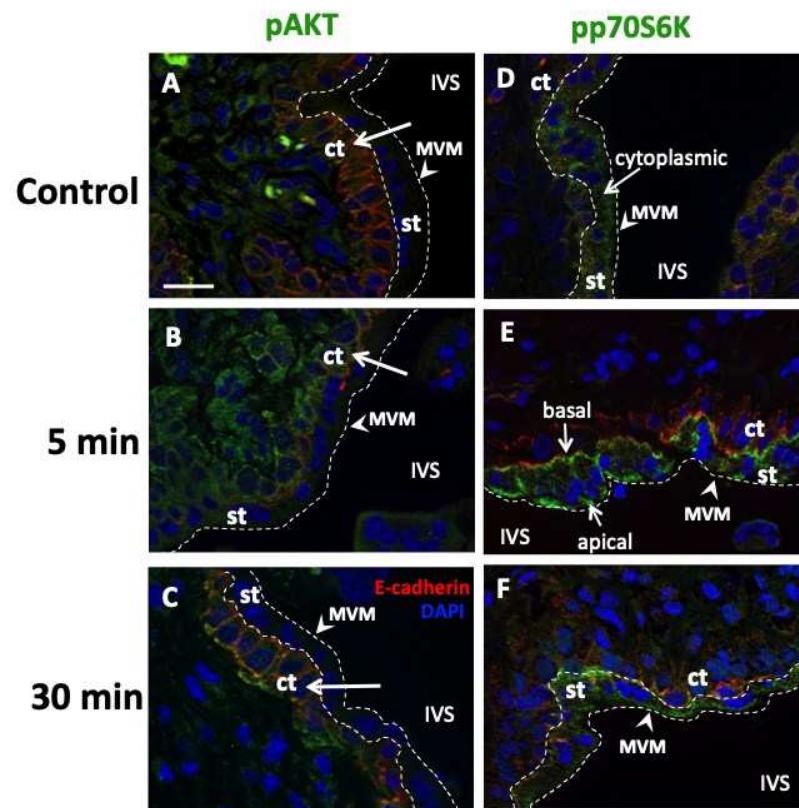


Figure 3: IGF-I activation of intracellular signalling molecules in human first trimester placenta. Treatment with IGF-I (20nM) for 5 and 30 min activates intracellular AKT, GSK and P70S6K signalling pathways. Phosphorylated AKT (pAKT; A-C, n=5) was observed only in cytotrophoblasts (green, indicated by arrow). IGF-I stimulation led to pP70S6K (green, n=3) translocation from cytoplasm to the apical and basal syncytial membranes (D-F). No activation of P70S6K was observed in cytotrophoblasts. st - syncytium, ct - cytotrophoblasts, also indicated by white arrows in A, B and C. MVM - microvillous membrane, IVS - intervillous space; E-cadherin, a cytotrophoblast marker (red); DAPI, nuclear stain (blue). Representative images from n=3-5 placentas. Syncytium is enclosed by white dashed lines in A,B,C and F. Only the apical microvillous membrane is dashed in B and E to avoid obscuring the staining. In E, the basal and apical syncytiotrophoblast are marked by arrows. Scale bar, 10µm.

254x338mm (72 x 72 DPI)

Figure 4

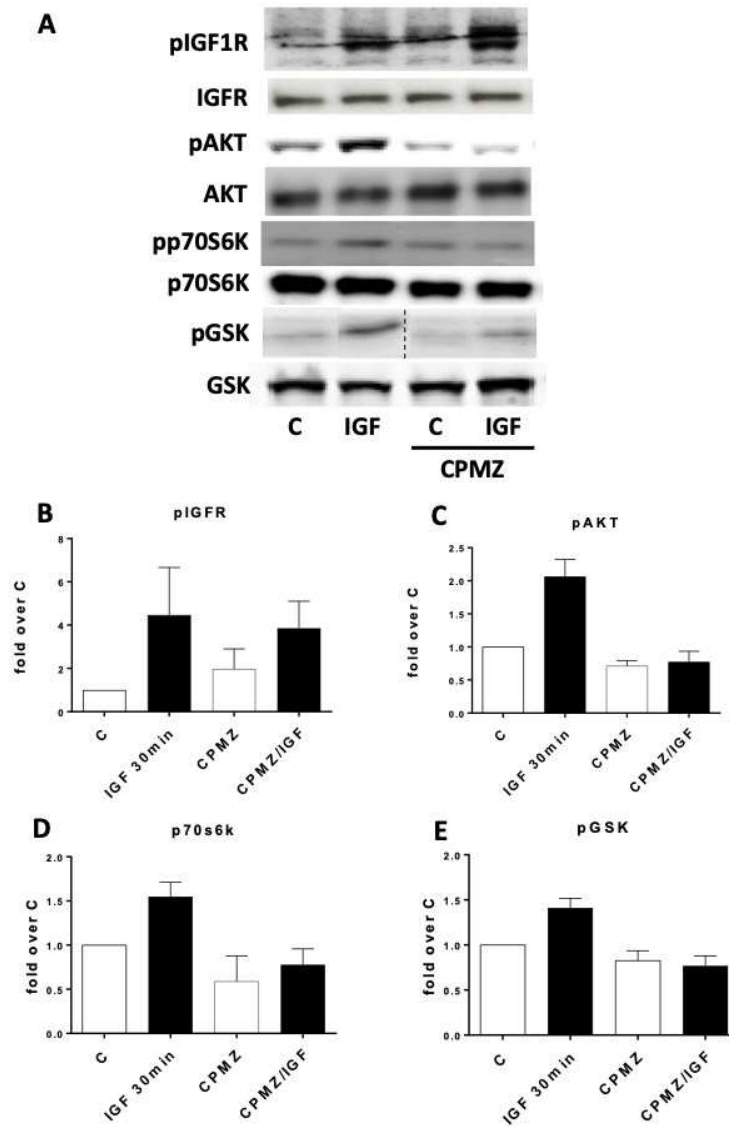


Figure 4. Clathrin-mediated endocytosis affects IGF-I induced signalling in human early placenta. Western blot analysis of first trimester placental explant lysates (A) demonstrates that treatment with IGF-I (20nM) for 30 min increases activation of IGF1R (B; $p=0.33$) and AKT (C; $p=0.38$); control (C) vs IGF. Pretreatment for 30 min with the clathrin-mediated endocytosis inhibitor, CPMZ (100 μ M), reduces IGF-I-stimulated phosphorylation of AKT (C; $p<0.0001$), P70S6K (D; $p=0.038$) and GSK (E; $p=0.003$), but does not affect phosphorylation of IGF1R (B; $p=0.99$); IGF vs IGF+CPMZ. $n=4$ for pIGF1R, $n=9$ for pAKT, $n=6$ for pp70S6K and $n=5$ for pGSK). Within each experiment, all samples were run on the same gel; however, we have rearranged some lanes (indicated by dotted line) from the resultant image of the autoradiograph in order to present the data in the sequence used to report all other results: control, IGF, control + CPMZ, and control + IGF. Each lane contains 20 μ g protein.

254x338mm (72 x 72 DPI)

Figure 5

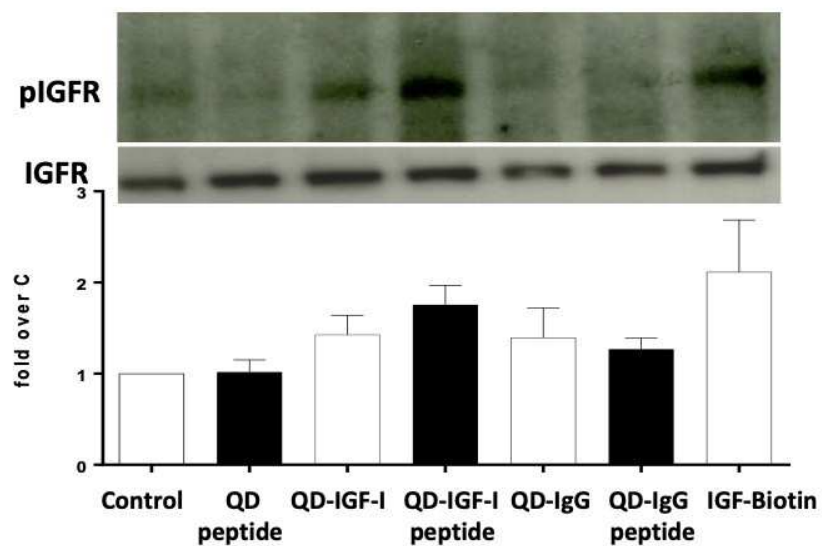


Figure 5. QD-IGF-I conjugates retain biological activity.

First trimester placenta was treated for 30 minutes with QD-peptide (iRGD), QD-IGF-I (100nM), QD-IGF-I-peptide (100nM), QD-IgG (100nM) or QD-IgG-I-peptide (100nM) (concentration in brackets refers to IGF-I final concentration). 50nM IGF-biotin was used as a positive control, and untreated tissue was used to define basal levels of IGF1R phosphorylation. Western blot analysis (20 μ g protein/lane) reveals an increase in pIGF1R following treatment with QD-IGF-I-peptide ($p=0.0004$, $n=6$) and IGF-I-biotin ($p=0.0005$, $n=4$).

254x338mm (72 x 72 DPI)

Figure 6

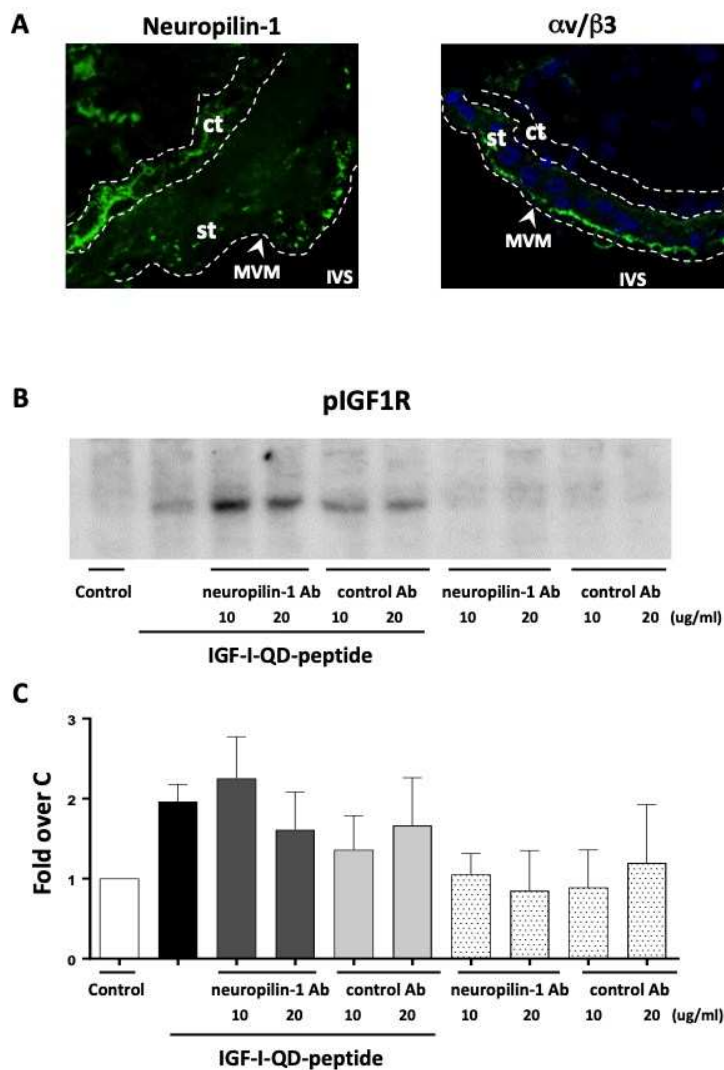


Figure 6. Blocking QD-IGF-I-peptide binding to neuropilin-1 increases phosphorylation of IGF1R. Neuropilin-1 (green) is present in both the MVM and the cytotrophoblast layer, whereas integrin $\alpha v/\beta 3$ (green) is present exclusively in the MVM in the first trimester placenta (A). MVM - microvillous membrane, IVS - intervillous space, st - syncytiotrophoblast, ct - cytotrophoblast. First trimester explants were treated with a control antibody or an antibody (10 or 20 $\mu\text{g/ml}$) specific to the neuropilin-1 iRGD peptide binding site for 1h, then incubated in the absence or presence of QD-IGF-I-peptide (iRGD) for 30 min. Activation of IGF1R was assessed by Western blotting (B). Control vs QD-IGF-I-peptide ($p=0.0099$; $n=6$) and control vs neuropilin/QD-IGF-I-peptide ($p=0.0295$; $n=3$). No difference was detected at the higher dose. Syncytium is enclosed by white dashed lines. The basal cytotrophoblast surface is also marked by a white dashed line.

254x338mm (72 x 72 DPI)

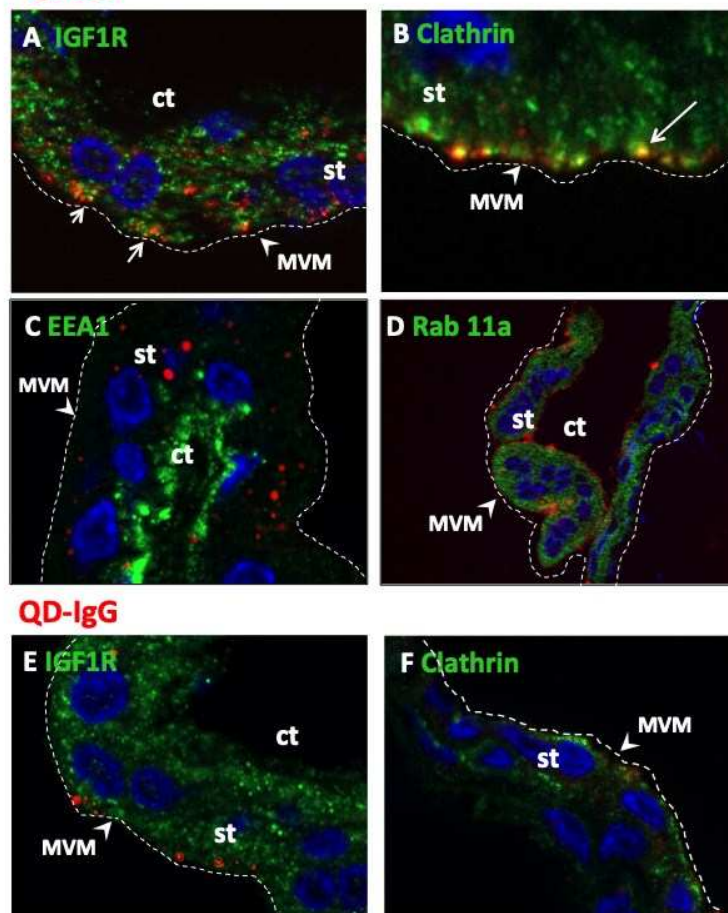
Figure 8**QD-IGF****QD-IgG**

Figure 8. Colocalisation of QD-IGF-I with IGF1R and endocytosis markers
QD-IGF-I (red) colocalised with IGF1R (A, green; arrow) and clathrin (B, green) close to the apical microvillous membrane (MVM) in the syncytial (st) but not cytotrophoblast layer (ct). This was not observed for the control QD-IgG (E and F). QD-IGF-I did not colocalise with the early endosomal marker EEA1 (C and D), or Rab11a (recycling endosome). Nuclei are stained with DAPI (blue). Representative images from n=3 placentas. White dashed lines delineate the apical syncytial microvillous membrane.

254x338mm (72 x 72 DPI)